# Heat Drain Device for Ultrasound Imaging Probes

L. Spicci, G. Vigna
Research and Development Department, Esaote S.p.A.,
Via di Caciolle 15, 50127, Florence, Italy.
lorenzo.spicci@esaote.com, giuseppe.vigna@esaote.com

**Abstract:** Ultrasound imaging probes are widely used for several types of diagnosis applications. Since the electroacoustic conversion efficiency of a probe is never 100% and in most cases the duration of clinical examination can be quite long, the surface temperature of the probe head, in contact with human body, must be kept under control. International Safety Standard EN 60601-2-37 [1] sets an upper limit for the surface temperature in still air of 50°C (43°C if measured when coupled thermally and acoustically with a test object having thermal and acoustical properties mimicking those of an appropriate tissue).
The temperature rise is caused mainly by joule heating effect inside the active piezo-transducer and could be very important under some operating conditions (i.e. Continuous Wave Doppler (CW); Pulsed Wave (PW) Doppler; Colour Flow Mapping (CFM)).
In the present work we focus our attention on a small footprint phased array probe. Temperature of the front face of the analysed probe must be reduced, because during CW and PW operating conditions it could exceed the limit imposed by International Safety Standard. We present here a detailed 3D FEM for the transducer , designed to replicate the real operation of the device and to be compared with measurement (electric and thermal) in order to optimize some key parameters of modelled materials. Then we show the way found to engage the thermal managing requirement, consisting in a very thin layer of super thermally conductive material that acts as heat drain toward a heat sink (in this paper it's avoided to give more detail on the name and characteristics of this material for confidentiality reason). Also in this case a comparison between FEM and measurements will be presented. In particular, we will show how the transducer performance, in terms of thermal response, changes by varying the conductive layer thickness. In conclusion, a possible future work, consisting in a FEM for the transducer with an additional dissipation system based on Phase Changing Materials (PCM), will be presented. The patent of the present invention is currently under submission.

**Keywords:** thermal analysis, ultrasound transducer, piezoelectricity, thermally conductive layer, FEM, COMSOL, PCM.

## 1 Introduction

Probes for diagnostic ultra-sonography application are devices that generate a pressure field into the human body, according to an electrical signal [1]. The efficiency of energy conversion, from applied electrical to stored mechanical one, is called (for a piezo-material) the *electromechanical coupling factor k* :

$$k^2 = \frac{mechanical\ energy\ stored}{electric\ energy\ applied} \quad \text{I.}$$

Since *k* is always lower than 1, a temperature rise for the probe head occurs.
The main cause of the temperature rise are the joule losses in the piezo-transducer with the dynamics of heating controlled by specific heat and thermal conductivity values for the materials used in the probe construction and the final steady state temperature of the probe surface depending mainly on the internal loss of the piezo-material and the electrical driving power.
As anticipated, the International Safety Standard EN 60601-2-37 [1] sets an upper limit for the surface temperature in still air of 50°C for whatever operating condition, in order to avoid patient discomfort. Such requirement should not be a limitation for the optimum power output of the transducer,. Indeed, the power limitation of the transducer output leads to a reduction of maximum temperature reached on the top of the transducer lens, but also reduce transducer performance in terms of imaging capability.
This issue has been engaged by the introduction of a very thin thermally conductive compound layer below the transducer silicone lens. In this way heat is drained on the back of the transducer where it can be dissipated by an adequate heat sink. The present thermally conductive

compound is a very effective material for this purpose, mainly for two reasons:

- It has acoustic properties that are similar to the silicone acoustic lens, so there is no efficiency loss.
- It has exceptionally high thermal conductivity (much more than metals, $\sim 4000\ \frac{W}{m \cdot K}$) so it is possible, even using a very thin layer, to achieve better heat drain results with respect to a thicker metal layer.

In Figure 1 a thermally conductive compound sample is shown.

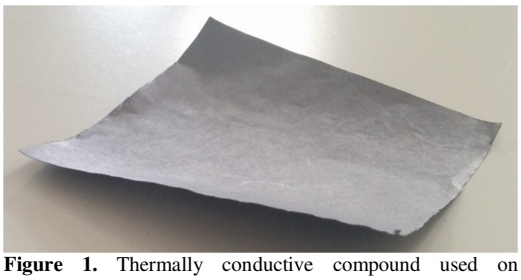

**Figure 1.** Thermally conductive compound used on transducer prototype.

## 2 Multiphysics FEM

We briefly describe here the essential model characteristics that are used for the present COMSOL FEM.
The multi-physics approach is required because both the piezoelectric and thermal effect are studied. In particular, the transducer is modelled using the "*acoustic-piezo-electric*" module and thermal effect is modelled using the *"heat transfer"* module. The acoustic-piezoelectric analysis has been made first (study 1), in order to use information concerning heat dissipation as input parameter for thermal analysis that has been later made (study 2).

### 2.1 Piezo-electric material modelling and electrical characteristics

The constitutive equations for a piezo-electric material are [2], in *stress-charge* form:

$$\text{II.} \qquad \begin{cases} \mathbf{T} = [\mathbf{c^E}]\,\mathbf{S} - [\mathbf{e}^t]\mathbf{E} \\ \mathbf{D} = [\mathbf{e}]\,\mathbf{S} + [\boldsymbol{\varepsilon}^S]\mathbf{E} \end{cases}$$

where **T** is the stress vector, **c** is the elasticity matrix, **S** is the strain vector, **e** is the piezo-electric matrix, **E** is the electric field vector **D** is the electric displacement vector, **ε** is the dielectric permittivity matrix. The superscripts indicate a zero or constant corresponding field.
Equation II takes into account both piezo-electricity, both mechanical and electrical anisotropy of the material.
From the electrical point of view, the electrical impedance $Z$ of a piezo-electric plate can be calculated from the potential difference $V$ and the flowing current $I$ across the plate faces. $V$ is impressed between the plate faces, while $I$ is calculated as surface integral of the current density component along $z$-axis.
The piezoelectric analysis has been carried out in frequency domain in order to have, as result, impedance curve versus frequency. Impedance analysis and optimization by comparison with measurement has been made in order to optimize material parameters and use the resulting power dissipation as heat source for thermal analysis (second stage).
The dielectric losses are specified for the piezo-material, so that the resulting heating effects are recalled in the heat transfer module as a power dissipation source.

### 2.2 Heat transfer modelling

The module of heat transfer in solids has been used to model heating in the present work. Heat transfer in solids is described by the following equation [2]:

$$\text{III.} \qquad \rho \cdot C_p \cdot \frac{\partial T}{\partial t} + \rho \cdot C_p \cdot \boldsymbol{u} \cdot \nabla T = \nabla \cdot (k \nabla T) + Q$$

where $\rho$ is the material density, $C_p$ is the material heat capacity, $k$ is the material thermal conductivity, **u** is the velocity field of fluid at fluid-solid interface and Q is a heat source. In the present model fluid-solid interface is not modelled, as we are not interested in the heat transfer in surrounding fluid (air) and need to limit the 3D model dimensions. Thus we used a convective heat flux boundary condition on surfaces on which convection is present. As regard the heat source, total power dissipation density of piezoelectric and other materials has been impressed. This value depends on the loss

factor for electrical permittivity set for the piezoelectric material (isotropic loss factor for others), and it has been optimized comparing FEM preliminary simulation results with corresponding measurement. Heat transfer analysis has been made in the time domain using as working frequency values of 2 and 5 MHz. Obviously heat dissipation of transducer depends on working frequency and the maximum value is reached when operating close to anti-resonance frequency [3]. On the other hand, the frequency values above correspond to the ones available on the imaging scanner.

### 2.3 FEM Mesh and transducer structure

The mesh used in the FEM was a physics controlled tetrahedral one. It has been not possible to satisfy the λ/10 rule (where λ is the minimum wavelength of interest) because of computing time restriction. However the model was validated through comparison with measurement. In Figure 2 and in Figure 3 the transducer components are briefly described in order to have a better overview. In Figure 4 and in Figure 5 the mesh used is represented.

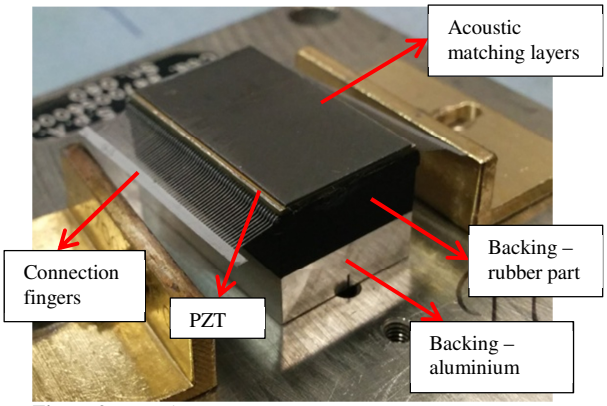


**Figure 2.** Transducer components

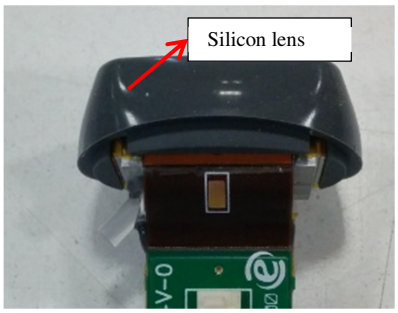


**Figure 3.** Transducer silicon lens

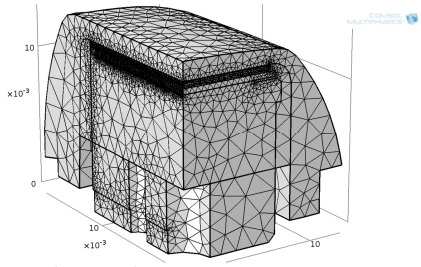

**Figure 4.** Transducer mesh

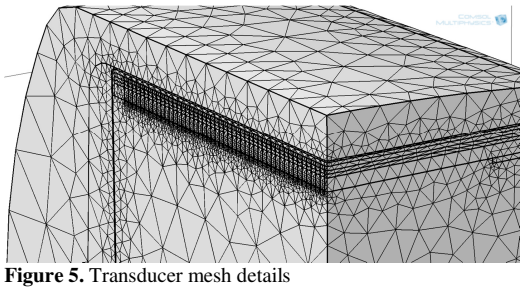

**Figure 5.** Transducer mesh details

### 2.4 Boundary conditions

The model has been limited to ¼ of the entire geometry in order to reduce computing time, making use of proper symmetry conditions.
As regard study 1 electrically boundary conditions are ground on top surfaces of PZT material and driving potential on the bottom. On study 2, as already mentioned, a heat source has been impressed on the entire volume, to take into account the heating resulting from all material losses. Moreover, surrounding air convection was considered as a heat flux boundary condition on all the external surfaces, with a value of heat transfer coefficient $h = 10\ W/(m^2 \cdot K)$. Such value was calculated from a previous simulation for a free convection cooling of a reference aluminum block.

## 3 Working Layout

The present work was developed following the steps listed below. Each step is designed, in order to analyse the most relevant performances of the described solution:

1. Acoustic-piezoelectric and thermal simulation results of the 3D FEM for the current standard production phased array transducer were compared with measurements on the real device, in

order to optimize the FEM in terms of all materials. This analysis has been made using a step by step approach [4] on each transducer manufacturing phase, in order to simplify the optimization process.

2. Acoustic and thermal simulation results of the 3D FEM for the modified phased array transducer, introducing the thermally conductive compound layer, were performed varying its thickness, in order to find the optimal value, representing a trade-off between acoustic performance and heat drain. A comparison between standard and modified transducer has been carried out by manufacturing prototypes and performing measures on both of them.

3. Thermal simulation results of a 3D FEM for a possible future work, corresponding to filling the internal probe cavity with a phase change material (PCM). This material has the capability to draw heat at a steady transition temperature, because it changes its physical state and store 'latent' heat.

### 3.1 Measurement equipment and FEM comparison

The transducer's basic performances can be evaluated by measurement of the electrical impedance; whose quality and reliability play an important role in the comparison with simulation results. For a complete transducer–performance analysis and optimization, we invite the reader to look at [3], [4].
Impedance measurement has been performed with Hewlett Packard 4195A Network Analyser.
As regard temperature measurements, the phased array transducer was powered with an Esaote scanner device that applies, at 5 MHz frequency, a driving voltage across the PZT poles. The voltage value changes with load changing, so it has been measured, at every step, in order to replicate that on the FEM. The transducer has been left to free convection on the sides and bottom surfaces and a type *k* thermocouple, applied on the top exposed surface (in the middle) has been used. The thermocouple head was coupled to the transducer surface with thermally conductive paste and the head dimensions was chosen to be less than 1 mm in order to get a negligible inertial thermal effect. Note that the *k* type thermocouple sensitivity of about 41 μV/°C is capable to describe with high accuracy also a very low thermal variation of the disk-probe. Thermal measurements where performed in a thermostatic environment at 25 °C using a specialized plexiglass box in order to avoid any additional and uncontrolled convective flux (Figure 6). Using the above set-up the uncertainty of the temperature measurement can be evaluated in ±1°C.

**Figure 6.** Specialized plexiglass box and measurement set.

### 3.2 Standard transducer characterization

The FEM optimization on transducer material has been performed on each manufacturing stage of the transducer, following the step approach method presented in [4]. The comparison has been made both in terms of electrical impedance, both in terms of temperature rise. Electrical impedance analysis allows to optimize PZT material parameters like elasticity matrix, coupling matrix, relative permittivity and also matching layers and backing elastic parameters (Young modulus, Poisson coefficient). Temperature analysis allows to optimize basically all material losses.
The first analysis step was the PZT plate with connection fingers soldered. The second step was the PZT bound on the backing support. Then

acoustic matching layers were added on top. Results for the latter comparison stage are reported in Figure 7 and Figure 8: agreement is considered very good.

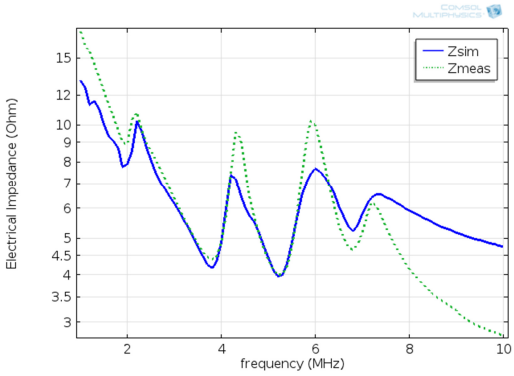


**Figure 7.** Transducer electrical impedance, comparison between measure and simulation.

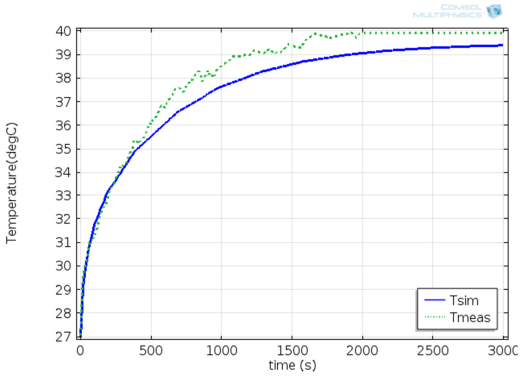


**Figure 8.** Standard transducer head temperature, comparison between measure and simulation.

The last stage corresponds to the complete transducer model. Transducer has been diced and the silicon lens has been added on the top. As a result of transducer dicing, resonance frequency is lowered down to approx. 2MHz, as it is possible to see in Figure 9. Complete transducer electrical impedance, comparison between measure and simulation., where a comparison between measurement and simulation in terms of electrical impedance is represented. Thus simulation and measurement has been performed at 2.1 MHz instead of 5 MHz as for the plate not diced. A comparison in terms of temperature has been performed and it is represented in Figure 10. The agreement between simulation and measurement is considered acceptable for our probe design purpose.

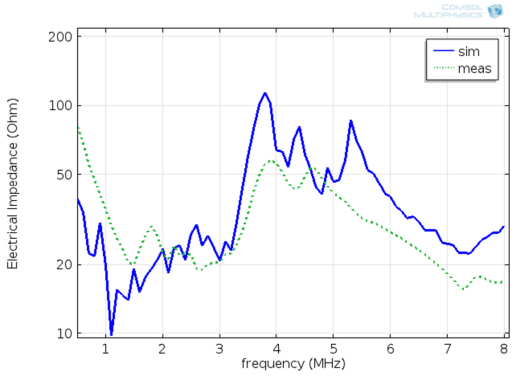


**Figure 9.** Complete transducer electrical impedance, comparison between measure and simulation.

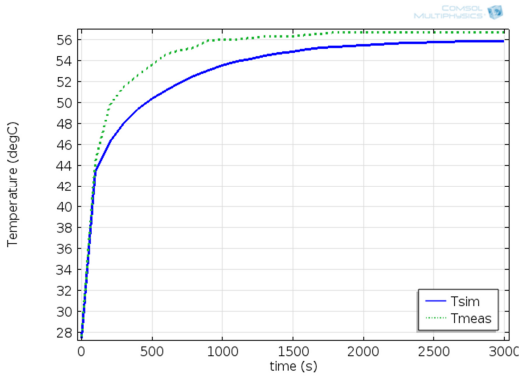


**Figure 10.** Standard transducer head temperature after dicing and lens bonding, comparison between measure and simulation.

### 3.3 Conclusions on standard transducer configuration

As shown in Figure 10 and Figure 11, the temperature of transducer reaches about 56 °C after 3000s for the standard design. Moreover, the 3D heat flux and temperature plot shows an uniform heating distribution, with no heat preferred path. This is not desirable as it should be better to have an heat drain channel toward a heat sink. To accomplish such goal a solution presented in the following paragraph has been developed.

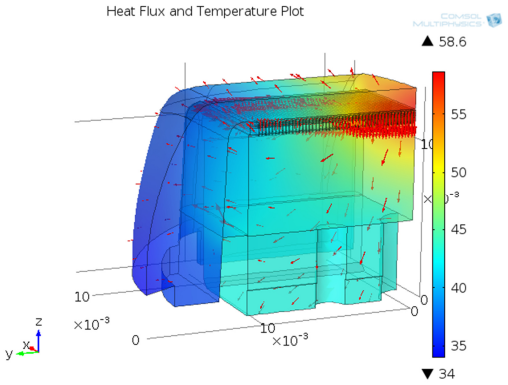


**Figure 11.** 3D plot of temperature and heat flux in the standard transducer.

## 4 Modified transducer characterization

The thermally conductive compound layer has been introduced between silicone acoustic lens and matching layers. The thermally conductive compound layer has been designed to contact and transfer heat to the aluminium part of the backing that could be used as a heat sink, thanks to the very high thermal conductivity of the compound material. This assumption is confirmed by results of FEM simulation compared with measurements (Figure 12). Here it is visible that maximum temperature is about 44°C after 3000s, so that it is reduced of about 12°C. In Figure 13 it is represented the 3D plot of temperature and heat flux. It is possible to see how heat flux is focused along thermally conductive compound layer instead of scattered as in the standard case.

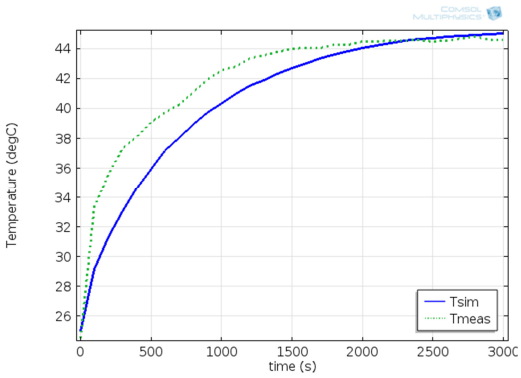


**Figure 12.** Modified transducer head temperature, comparison between measure and simulation.

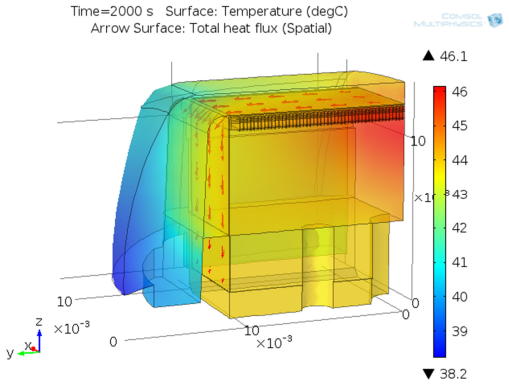


**Figure 13.** 3D plot of temperature and heat flux in the modified transducer.

### 4.1 Conclusions on modified transducer configuration

It is possible to conclude that the thermally conductive compound layer represents a concrete solution for heating issues of an ultrasound transducer. FEM and measurements match well and this allows to proceed to the next step of this work.

## 5 Thermally conductive compound layer thickness influence on transducer thermal performance

After previous FEM validation and study, it is possible to carry out an analysis on thermally conductive compound layer thickness optimization. As mentioned before, thermally conductive compound layer thickness must be as low as possible in order to be “invisible” to acoustic wave. An analysis of transducer thermal performance has been carried out varying thermally conductive compound layer thickness from 0.05 mm down to 0.02 mm. In Figure 14 a comparison of temperature vs time curve relative to these two different analysis is represented. It is possible to see that as thermally conductive compound layer thickness is lowered, the final transducer temperature rises. This means that thermally conductive compound thickness layer must be optimized to reach a trade-off between thermal and acoustical performance.

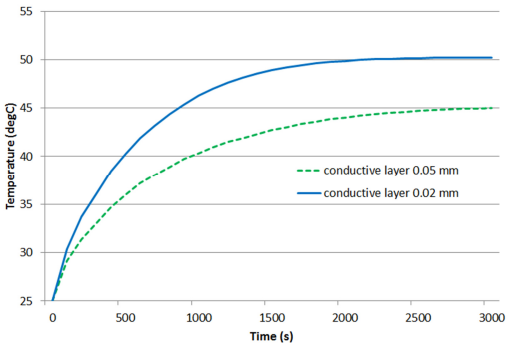


**Figure 14.** Transducer head temperature dependence on thermally conductive compound layer thickness.

## 6 Additional dissipation system (future work)

To complete a reliable cooling system it is important to consider a better heat sink device on the rear part of the transducer. Indeed the transducer will be closed and sealed inside the probe plastic handle, so it is not possible to rely on heat convection by air as efficient cooling effect. The approach described in this paragraph is based on the use of an ideal Phased Change Material (PCM). As mentioned before, the phase change material compound will be placed in the rear part of the probe, in order to draw heat at a steady transition temperature, as it changes its physical state and store 'latent' heat. This will keep the probe temperature constant during the PCM phase change. As a first approach on this study, a simulation has been carried out by imposing a very high heat flux coefficient ($h_{PCM}$) on the backside of the transducer at the PCM transition temperature ($T_{trans.}$), in order to simulate an infinite heating dissipation based on the equation IV:

$$\text{IV.} \qquad Q_{PCM} = h_{PCM} \cdot (T_{trans.} - T)$$

where the following values has been used:

$h = 1 \cdot 10^5 \ W/(m^2 \cdot K)$ and $T_{trans.} = 33\ °C$ .

In Figure 15 the plot of transduced head temperature vs time is represented. Since an ideal PCM has been modelled, the temperature of the probe head is kept constant to a value slightly higher than $T_{trans}$ corresponding to the equilibrium temperature of the entire system . It is possible to conclude that this kind of solution helps to reduce the transducer temperature, so next study could be focused on the PCM optimization inside the transducer. Such optimization should deal with the study of the best values for the $T_{trans}$ and PCM storage capability inside the probe.

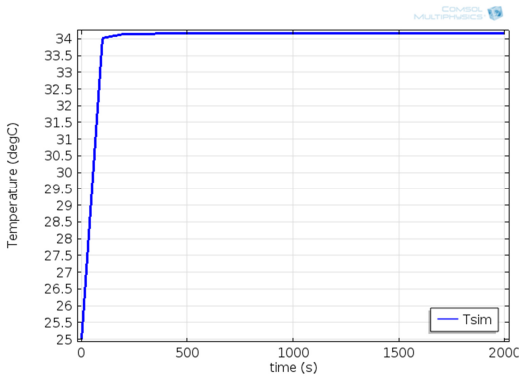


**Figure 15.** Head temperature of a transducer filled with an ideal PCM.

## 7 Conclusion

A cooling system for an ultrasound transducer was designed and developed along with the corresponding COMSOL FEM. At the current development stage it is already possible to lower the transducer temperature by 12 °C. The FEM can be used for further system optimization and upgrades.

## 8 References

[1] EN 60601-2-37, *"Medical electrical equipment - part 2: particular requirements for the safety of ultrasonic medical diagnostic and monitoring equipment"*.

[2] COMSOL Multiphisics Acoustic Module User Guide, ver.3.5a, pages 32-33.

[3] L. Spicci, M. Cati, *"Thermal Analysis of a piezo-disk ultrasound probe"*, Comsol Conference 2012, Milano.

[4] L. Spicci, M. Cati, "*Ultrasound Piezodisk Transducer Model for Material Parameter Optimization*", Comsol Conference 2010, Paris (best paper award).